

Are All-speed Density Based Solvers Required for RANS of Compressible Boundary Layers?

B. Thornber

School of Aerospace, Mechanical and Mechatronic Engineering, The University of Sydney, Sydney, New South Wales, 2006, Australia

Abstract

Standard compressible flow solvers lose accuracy at low Mach numbers as they become excessively dissipative. This dissipation can be reduced by either refining the mesh significantly, or by utilising an all-speed scheme. This paper explores whether the use of an all-speed scheme is required to accurately resolve a compressible turbulent boundary layer at low Mach, using a truncation error analysis. Taking Mach 0.1 as the starting point, it is shown firstly that an attached boundary layer is not a challenging configuration even for first order accurate schemes. In regions of separation numerical dissipation increases dramatically, and a second order scheme is likely to provide numerical dissipation close to that given by the turbulence model. In such a situation, the corrected scheme would be advantageous, but for simple attached boundary layers such a correction would not be required.

Introduction

Several all-speed algorithms have been proposed recently which aim to extend the applicability of upwind (density-based) methods to low Mach flows, or mixed low/high Mach flows. These methods do not usually aim to address the stiffness or cancellation problems at low Mach [19, 12], but significantly improve the accuracy. Examples of these algorithms include a structured Godunov approach [16, 17], unstructured Godunov approaches [2, 1, 9], the SLAU flux [13], the AUSM+-up scheme ([7], and all-speed Roe schemes [15, 10, 3, 6]. Multiple previous papers have demonstrated the improvement in flows where the Mach number is clearly low ($M \ll 0.1$), however it is not clear if there is benefit in using an all-speed scheme when simulating boundary layers where the freestream Mach $M > 0.1$.

It is possible that the strong refinement within the boundary layer already reduces the numerical dissipation sufficiently thus giving negligible difference between the all-speed and the standard scheme. This was noted recently when simulating shock boundary layer interactions (SBLI) using Reynolds-Averaged Navier-Stokes (RANS) in supersonic flows [4]. It is also possible that the role of numerical dissipation in that problem was simply negligible in determining the details of the SBLI, so that the improvements in behaviour were simply not noticed. This short paper explores the variation of numerical dissipation within a typical flat plate boundary layer as both freestream Mach number and Reynolds number vary, for grids constructed for use with RANS. It starts by outlining the key assumptions in this analysis, then presents the results of the analysis of dissipation rate for boundary layer Reynolds numbers of 10^6 , 10^7 and 10^8 and finally draws the conclusions from the study.

Assumptions

This paper focuses purely on direction split Godunov-type methods. A typical example is a curvilinear multiblock compressible solver utilising MUSCL reconstruction [20] feeding into a HLLC approximate Riemann solver [18], such as that developed by the author [4]. The advantage of considering these schemes is that their multidimensional implementation is

a simple extension of the one dimensional method by conducting three one dimensional sweeps. Thus analyses can focus on the one dimensional problem which, once understood, also describes the performance of the three dimensional algorithm.

Dissipation Rate

It was shown that the dissipation of turbulent kinetic energy in a numerical scheme can be effectively determined by measuring the change in temperature multiplied by the entropy change during the simulation [16]. This applies to all numerical schemes, however the paper focused on deriving explicit leading order dissipation terms for a first order in time and space Godunov-type algorithm at low Mach. For example, the dissipation of kinetic energy in a standard explicit first order Godunov approach for a step change in velocity is [17],

$$\varepsilon \approx \frac{\Delta u^2 a}{4\Delta x} (1 - C), \quad (1)$$

where Δx is the grid spacing, Δu the velocity jump at the cell interface, a the speed of sound and C is the Courant-Friedrichs-Lewy number. The problem of standard compressible schemes at low Mach is that this dissipation rate increases linearly with a thus giving an unphysically high dissipation rate at low Mach.

To be Mach independent, the dissipation rate should scale with u^3/l where l is a typical length scale. If this length scale is assumed constant, then the any decrease in Mach number must be accompanied by an increase in mesh resolution to maintain accuracy. For example, if the Mach number of a first order accurate scheme is reduced by a factor of 10, then for an uncorrected scheme the mesh spacing Δx must decrease by a factor of 10 in each direction to maintain accuracy. With a low Mach correction, this is not necessary.

In a boundary layer, the length scale that is resolved in the computation depends either on the curvature of the mean flow (RANS), the thickness of the boundary layer (RANS), or on the local eddy size (LES/DNS). It is normal practice to cluster the points close to the wall, which would naturally reduce dissipation, thus at a high enough Mach number the clustering may be sufficient to gain the necessary reduction to maintain the accuracy of the scheme (in the wall normal direction).

To determine this, a more general form of equation(1) is required for smoothly varying flows. Following the analysis of [16] but using a continuous function instead of a step, and assuming constant pressure and density initially, the leading order kinetic energy dissipation rate is

$$\varepsilon = \frac{\Delta x (a^2(1 - C) + CU^2) U_x^2}{2a} \quad (2)$$

This expression has been validated through an unsteady test case with the following initial conditions solved on a domain of size 1,

$$p = p_0/M^2, \quad \rho = \rho_0, \quad u = 0.5Ma \sin(2\pi x), \quad (3)$$

where the Mach number $M = 0.01$.

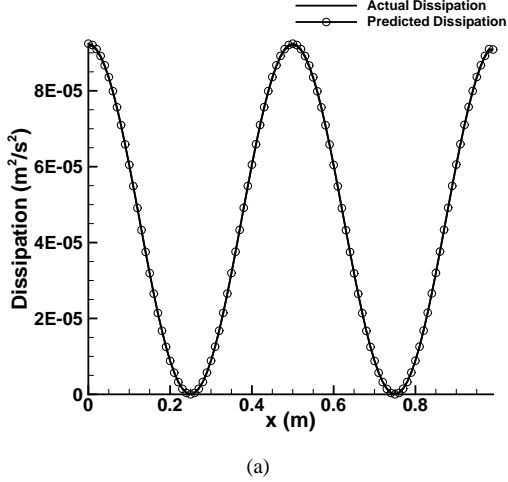


Figure 1: Actual dissipation of kinetic energy over a single time step compared to predicted using equation (2) for a testcase consisting of a simple sinusoidal flow field

Figure 1 compares the entropy rise over one time step for each cell as predicted by equation (2) and calculated from the simulation. This equation is predictive - it matches actual cell-by-cell numerical results to within 1% at Mach 0.01, which in the authors knowledge is the first time a validated and accurate quantitative formula predicting the dissipation rate of a fully compressible Godunov scheme has been presented. It will be used here to give predictions for the flat plate boundary dissipation rate, where the key assumption is that pressure is constant and density gradients low, thus entropy production will be driven by the velocity gradients.

Note also that previous studies showed that the only component of the dissipation which increases as Mach decreases is that due to the interface-normal velocity component, the dissipation of shear waves is Mach uniform [17].

Grid Resolution and Boundary Layer Profile

Typical RANS grids place the first point at $y^+ = 1$ (wall resolved low Reynolds), or $y^+ \approx 50$ (wall modelled). The cells are grown using a growth factor of 1.2 up to a maximum of $\delta/10$ and then remain of a constant size, where δ is the local boundary layer momentum thickness [14]. A relatively fine resolution of $\Delta x^+ = 100$ in the streamwise direction is assumed here. These criteria will be employed in the analysis presented here.

The mean boundary layer velocity profile is modelled by a linear viscous sublayer where $u^+ = y^+$ for $y^+ \leq 11$, a log-law region $u^+ = 2.44 \ln y^+ + 5.2$ up to $y = 0.1\delta$ and an outer region where the log law is linearly blended with a one-seventh power law $u^+ = U_e/u_\tau(y/\delta)^{1/7}$ up to $y = \delta$ where the freestream velocity is achieved. The result is not expected to be overly sensitive to the exact details of the wall boundary layer model.

An important result to note is that even at $Re_x = 10^8$ at $M = 0.1$, the expected mean flow Mach number on the boundary of the viscous sub-layer is $\approx 37\%$ of the mean flow Mach - i.e. the gradient of the Mach number is relatively low through the boundary layer until the viscous sublayer. This implies that even at

$M = 0.1$ there is a good chance that increasing grid resolution will be sufficient for an attached boundary layer.

An effective numerical simulation should ensure that the numerical dissipation rate is below that expected physically, or provided by the turbulence model. In the case of a turbulent boundary layer, the dissipation provided by the turbulence model should be $\epsilon^+ = 1/\kappa y^+$ in the log layer [21]. Measurements indicate that this decreases to zero through the viscous sublayer where it is given by $\epsilon^+ = y^+/100$, and the intersect of these two curves is at $y^+ = 15.6$. In the subsequent section this provides the reference level of turbulent dissipation rate which the numerical dissipation rate should be significantly below.

Using this foundation, the next section explores the variation of dissipation rate within a typical boundary layer for RANS in the wall-parallel (x, z) and wall-normal direction (y). This paper starts at Mach 0.1, as below a freestream Mach number of 0.1 it is clear that the low Mach correction should be applied as has been shown in several previous test cases (see literature referred to in the introduction). If the dissipation rate is sufficiently low at Mach 0.1, then higher Mach numbers can be assumed to be sufficiently well resolved too.

Results

Examining the magnitude of the terms in the mean turbulent boundary layer equations [11], it is clear that the two principle sources of dissipation to consider in the solution of the inviscid part of the mean governing equations are those fluxes due to (i) streamwise gradients ($\rho u \partial u / \partial x$) and (ii) advection of shear gradients ($\rho v \partial u / \partial y$), which are both of order 1 in the boundary layer equation for streamwise momentum.

The maximum streamwise gradient based on the model mean boundary layer equation is at the boundary layer edge, where $\partial u / \partial x = (-6/49)U/x$ where x is the length of the boundary layer up to that point. The streamwise gradient decreases approximately proportional to $y^{1/7}$ towards the wall and can be written as $\partial u / \partial x = \frac{-6/49}{U} \left(\frac{y}{0.16} \left(\frac{U}{v} \right)^{1/7} \right)^{1/7} x^{-55/49}$. For a first order accurate scheme without a low Mach correction the leading order kinetic energy dissipation rate is given by equation (2), accurate to within a percent. Combining this result with the empirically defined u_x gives the result that with constant streamwise grid spacing through the boundary layer the numerical kinetic energy dissipation rate decreases through the boundary layer proportional to $y^{2/7}$.

The numerical dissipation for the 1st order scheme is plotted with the expected turbulent dissipation rate ϵ in Figure 2 (a) for three representative Reynolds numbers at $M_\infty = 0.1$. The dissipation due to the streamwise gradients is several orders of magnitude below the dissipation of the turbulence model for the majority of the boundary layer for $10^6 \leq Re_x \leq 10^8$, due to the slow rate of change of the streamwise gradients. With curvature the actual resolution required will increase, however under the assumption that the curvature of the mean flow is adequately resolved by the Δx^+ at the outer layer, the same Δx^+ will give sufficient levels of dissipation through the boundary layer even with a first order standard compressible scheme. This clearly implies that higher order schemes will equally have sufficiently low dissipation due to streamwise fluxes, even without a low Mach correction.

In a finite volume density based solver the term (ii) $\rho v \partial u / \partial y$ is represented as a transport of a shear wave in u by the wall normal velocity v over an interface oriented in the y -direction. As shown previously [17], the dissipation of this shear wave is uniform with respect to Mach number. The main requirement

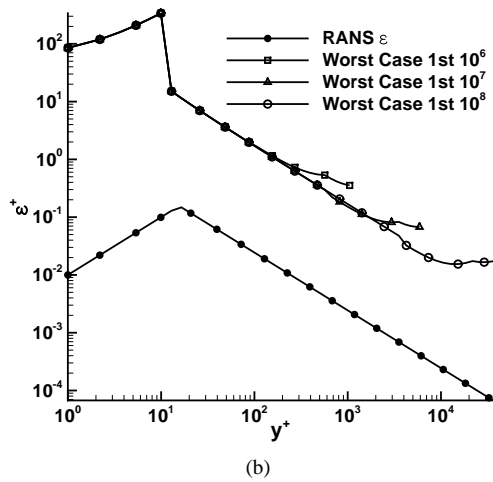
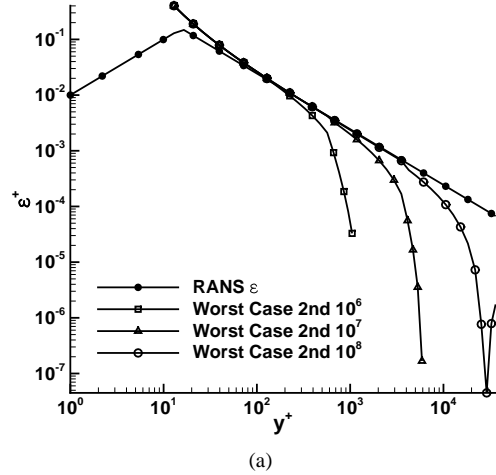
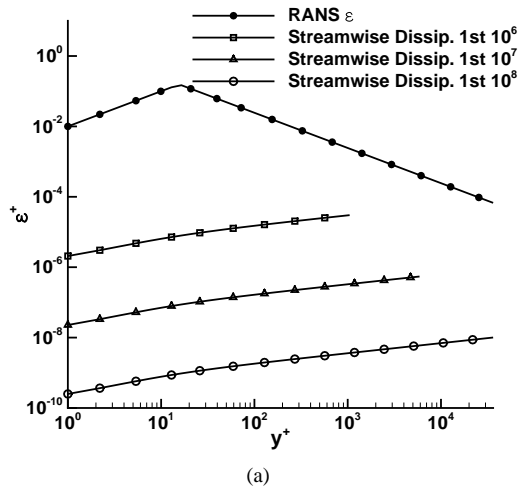


Figure 2: Dissipation rate due to (a) streamwise gradients at 1st order and (b) the worst case scenario of wall normal gradients aligned with the local velocity at 1st order scheme.

here is that the numerical scheme resolves the steeper gradients close to the wall which is satisfied for standard second order or higher schemes on meshes which follow the standard gridding guidelines (i.e. cluster to the wall).

The conclusion of this analysis is that a standard, uncorrected density-based scheme will be sufficient for attached boundary layers. For separation bubbles the gradients will change as the v velocity will now be of a similar order as the u velocity, invalidating the assumptions of the previous analysis. The worst case scenario is that the largest gradients are aligned in the direction of the smallest velocity. The largest gradient is $\partial u / \partial x = u_{\tau}^2 / \nu$ and is located in the viscous sub-layer.

Figure 2(b) illustrates the expected kinetic energy dissipation rate ϵ from the RANS model compared to the analytically predicted dissipation rate from the first order scheme assuming that both the velocity field and the gradients are directed in the wall normal direction. The first order scheme is at least two orders of magnitude too dissipative in this worst case scenario. This indicates clearly (i) a flat plate boundary layer is not a demanding test case, and (ii) numerical dissipation rates can be expected to change by five orders of magnitude in the region of a separation.

As effective RANS simulations typically employ second order accurate methods, it is important to extend these results to a

Figure 3: Dissipation rate due to the worst case scenario of wall normal gradients aligned with the local velocity with a 2nd order scheme compared to the expected turbulent kinetic energy dissipation rate ϵ^+ .

representative second order in space scheme. The MUSCL scheme with the second order upwind van Leer limiter is one such scheme. Rider and Margolin [8, 5] derived the effective numerical shear stress τ_{num} for the 2nd order van Leer limiter [20], however the expressions presented are too complex to be of use predictively.

Thornber *et al.* [16] presented the leading order terms for van Leer couple with a first order in time scheme. However, on closer inspection this term shows that this 2nd order in space/1st order in time system is actually marginally unstable, which is easily confirmed through computation. Extending this analysis to second order in time introduces a larger stencil and the resulting solution again becomes too complex to be of direct use. Thornber *et al.* also used numerical tests to demonstrate that for second order in space scheme with higher order accurate methods in time (i) ϵ scales with the speed of sound as shown for first order schemes, and (ii) it scales with Δx^3 which is the magnitude of the differences in the Riemann problem.

A leading order expansion for a second order scheme, similar to equation (2) is beyond the capabilities of current symbolic manipulation packages, where a simplified form has not been found. Using the testcase outlined in the assumptions section, the magnitude of the dissipation rate is reasonably well estimated by $\epsilon = \Delta x^3 a (1 - C) U_{xx}^2 / 4$ - however pointwise it is only accurate to the order of magnitude. Here it will be used to estimate the dissipation rate for the second order van Leer method applied to the model turbulent boundary layer.

Figure 3 shows the above worst case scenario plotted for the 2nd order van Leer scheme. The numerical dissipation rate is substantially reduced compared to the first order scheme as expected. However, it is still on the same order of the magnitude of the turbulent dissipation rate for much of the inner log layer. In the outer log layer, the numerical dissipation is lower, and in the viscous sublayer the theoretical error is zero as this is a second order scheme fitting a linear profile exactly.

Enabling the low Mach correction would reduce dissipation by a factor of 10 in this Mach 0.1 case to be $\approx 10\%$ of the expected turbulent dissipation rate at all points in the boundary layer. Note that in the worst case scenario depicted here, the expected turbulent dissipation rate will also be higher than that

plotted here for an attached smooth boundary layer.

Thus in regions of strongly varying flow properties, e.g. flow separations, then it is expected that a second order accurate standard density based compressible method will provide a dissipation rate which adds considerably to the turbulence model. With a low Mach correction, the dissipation rate due to the turbulence model would dominate.

Based on this analysis, it is likely that very high order schemes (e.g. fifth order) will not benefit greatly from the application of a low Mach correction at freestream Mach numbers greater than 0.1, should the standard grid resolution requirements be followed. It is worth noting that in practical geometries where the freestream Mach number is high, there are usually many regions where relatively low Mach number flows exist (e.g. secondary recirculation zones in flap gaps, or behind slats) and as such these would clearly benefit from a low Mach correction.

Conclusions

The above analysis has demonstrated through a quantitative analysis of first order and second-order accurate schemes that for RANS simulations of low Mach boundary layers ($M \approx 0.1$) and attached boundary layers a low Mach correction is likely not required. The dissipation rates predicted due to the Mach sensitive dissipation terms are substantially lower than the dissipation rates provided by the RANS model, even for a first order scheme.

An exploration of the worst case scenario indicates that the situation changes dramatically, with first order schemes certainly too dissipative, and second order schemes estimated to give dissipation of approximately the same order of magnitude as the modelled dissipation rate. Based on these observations, a benefit will be shown in employing a low Mach corrected second order scheme for more complicated flow fields. This scenario is representative of the conditions present in flow separation.

Given that the low Mach correction is computationally inexpensive (2% additional time), and that for geometries of practical interest there are usually several recirculation zones at considerably lower Mach than the freestream velocity, the rationale for a Mach-uniform algorithm is clear.

References

- [1] Dellacherie, S., Analysis of Godunov type schemes applied to the compressible euler system at low Mach number, *J. Comput. Phys.*, **229**, 2010, 978–1016, doi:10.1016/j.jcp.2009.09.044.
- [2] Dellacherie, S., Omnes, P. and Rieper, F., The influence of cell geometry on the Godunov scheme applied to the linear wave equation, *J. Comput. Phys.*, **229**, 2010, 5315–5338, doi:10.1016/j.jcp.2010.03.012.
- [3] Fillion, P., Chanoine, A., Dellacherie, S. and Kumbaro, A., FLICA-OVAP: A new platform for core thermal-hydraulic studies, *Nucl. Eng. Des. (in press)*, doi:10.1016/j.nucengdes.2011.04.048.
- [4] Garcia-Uceda Juarez, A., Raimo, A., Shapiro, E. and Thornber, B., Steady turbulent flow computations using a low Mach fully compressible scheme, *AIAA J.*, 1–17, doi:10.2514/1.J052948.
- [5] Grinstein, F., Margolin, L. and Rider, W., editors, *Implicit Large Eddy Simulation: Computing Turbulent Fluid Dynamics*, Cambridge University Press, Cambridge, 2007.
- [6] Li, X. and Gu, C.-W., Mechanism of Roe-type schemes for all-speed flows and its application, *Comput. Fluids*, **86**, 2013, 56–70.
- [7] Liou, M.-S., A sequel to AUSM, part II:AUSM+-up for all speeds, *J. Comput. Phys.*, **214**, 2006, 137–170.
- [8] Rider, W. and Margolin, L., From numerical analysis to implicit subgrid turbulence modelling, *AIAA 2003-4101*.
- [9] Rieper, F., On the dissipation mechanism of upwind-schemes in the low Mach number regime: A comparison between Roe and HLL, *J. of Comput. Phys.*, **229**, 2010, 221 – 232.
- [10] Rieper, F., A low-Mach number fix for Roes approximate Riemann solver, *J. of Comput. Phys.*, **230**, 2011, 5263 – 5287.
- [11] Schlichting, H., *Boundary-Layer Theory*, McGraw Hill, New York, 1979.
- [12] Sesterhenn, J., Muller, B. and Thomann, H., On the cancellation problem in calculating compressible low Mach number flows, *J. Comput. Phys.*, **151**, 1999, 597–615.
- [13] Shima, E. and Kitamura, K., Parameter-free simple low-dissipation AUSM-family scheme for all speeds, *AIAA J.*, **49**, 2011, 690–696.
- [14] Spalart, P., Young-person’s guide to detached-eddy simulation grids, Technical report, NASA, 2001.
- [15] Thornber, B. and Drikakis, D., Numerical dissipation of upwind schemes in low Mach flow, *Int. J. Numer. Meth. Fluids*, **56**, 2007, 1535–1541, doi:10.1002/fld.1628.
- [16] Thornber, B., Drikakis, D., Williams, R. and Youngs, D., On entropy generation and dissipation of kinetic energy in high-resolution shock-capturing schemes, *J. Comput. Phys.*, **227**, 2008, 4853–4872, doi:10.1016/j.jcp.2008.01.035.
- [17] Thornber, B., Mosedale, A., Drikakis, D., Youngs, D. and Williams, R., An improved reconstruction method for compressible flows with low Mach number features, *J. Comput. Phys.*, **227**, 2008, 4873–4894, doi:10.1016/j.jcp.2008.01.036.
- [18] Toro, E., *Riemann Solvers and Numerical Methods for Fluid Dynamics*, Springer-Verlag, Cambridge, 1997.
- [19] Turkel, E., Fiterman, A. and van Leer, B., *Preconditioning and the limit of the compressible to the incompressible flow equations for finite difference schemes*, John Wiley and Sons, 1994.
- [20] van Leer, B., Towards the ultimate conservative difference scheme.IV. A new approach to numerical convection, *J. Comput. Phys.*, **23**, 1977, 276–299, doi:10.1016/0021-9991(77)90094-8.
- [21] Wilcox, D., Turbulence modelling for CFD, *DCW Industries. California, USA*, **1**.